Stimulated spin-flip Raman scattering in a $Pb_{0.88}Sn_{0.12}Te$ single crystal

K. Yasuda and J. Shirafuji

Department of Electrical Engineering, Faculty of Engineering, Osaka University, Suita, Osaka 565, Japan
(Received 12 June 1978; accepted for publication 23 February 1979)

Stimulated spin-flip Raman emission assisted by resonance enhancement has been observed in an n-type $Pb_{0.88}Sn_{0.12}Te$ single crystal pumped by a TE CO_2 laser. The wavelength of the Stokes emission can be tuned in a range from 10.8 to 11.8 μm for the pumping wavelength at 10.54 μm in the magnetic field range between 8 and 40 kG. The effective g value, when a magnetic field is applied along the $\langle 100 \rangle$ axis, is from 50 to 64, depending on the magnetic field. The intensity of the Stokes emission is strongly dependent upon the magnetic field.

PACS numbers: 42.65.Cq, 42.55.Px, 78.45. + k

A spin-flip Raman (SFR) laser[1,2] has been first realized in an InSb cavity pumped by a Q-switched CO_2 laser. cw operation of the InSb SFR laser[3] has been achieved in a 5-μm range by a CO laser pump under the resonant Raman condition. The cw laser action in the 10-μm range (CO_2 laser pump) has been predicted in Ref. 2 by using a $Hg_{1-x}Cd_xTe$ or $Pb_{1-x}Sn_xTe$ cavity with suitable composition at the energy gap, which corresponds with pump radiation. Recently, the cw SFR laser using $Hg_{0.77}Cd_{0.23}Te$ cavity[4,5] has been achieved in the 10-μm range. In this note the first observation of the stimulated SFR emission assisted by resonance enhancement in a $Pb_{1-x}Sn_xTe$ crystal pumped by a TE CO_2 laser is presented.

An n-type $Pb_{0.88}Sn_{0.12}Te$ single crystal with a carrier density of 10^{17} cm^{-3} at 77 K was used as the SFR cavity. The energy gap of the crystal is estimated to be 122 meV at 10 K. The typical dimensions of the cavity were $5\times4\times3$ mm^3, where 5×4-mm^2 faces were mirror polished with 0.3-μm alumina abrasive. The parallelism of these two faces was within 12′, which was not satisfactory for good performance of the SFR laser. The cavity crystal was mounted and cooled to 10 K in an optical cryostat with a superconducting solenoid operating up to 50 kG. The optical pumping was made by a pulsed TE CO_2 laser operating at a single wavelength selected by an intracavity grating. The wavelength of the pump was varied discretely from 10.54 to 9.6 μm. This wavelength range can cover photon energies to induce the resonant Raman effect in the cavity. The incident CO_2 laser beam was focused onto the SFR cavity through a BaF_2 window of the cryostat by a KRS-5 lens with a focal length of 15 cm. The focused area of the pumping beam on the cavity surface was about 3 mm^2. The incident pumping beam and magnetic field was arranged in the Voigt configuration, and the $\langle 100 \rangle$ axis of the crystal was parallel to the magnetic field. The collinear SFR radiation was separated from the pumping light through a conventional grating monochromator and detected by a Ge : Hg photoconductive cell cooled to 30 K. The output signal from the detector was averaged with a boxcar integrator. The lowest detection limit of the present system was about 10 μW/cm^2.

The intensity of the stimulated emission was found to be dependent upon the intensity and wavelength of the pumping light, and the magnetic field. When the Raman cavity under the magnetic field of 16 kG was excited by the 10.54-μm light, the Stokes-Raman output became detectable at a pumping intensity of 0.6 MW/cm^2 and then steeply increased with increasing pump intensity, as shown in Fig. 1. This rapid increase in the output power with the pump power and, in addition, the sharp directionality of the output light beam indicate the stimulated nature of the SFR emission. However, the conversion efficiency defined as the Stokes power per unit pump power was extremely low at the present stage of the experiment. At a pump power of 7 MW/cm^2, the maximum output attained was only 6.6 mW, corresponding to the conversion efficiency of 3×10^{-6}%. Patel and Shaw[2] have estimated the SFR gain for unit incident power density, without a resonance enhancement effect in PbTe, to be about 10^{-5} cm^{-1}/W cm^{-2} when the magnetic field is applied parallel to the $\langle 100 \rangle$ axis. Assuming a maximum SFR gain in the present $Pb_{0.88}Sn_{0.12}Te$ cavity to be 10^{-5}

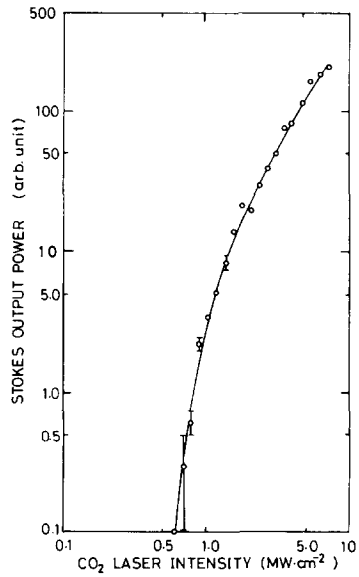

FIG. 1. Stokes output power as a function of pump power for the pump wavelength at 10.54 μm and a magnetic field of 16 kG.

 0003-6951/79/100661-03$00.50

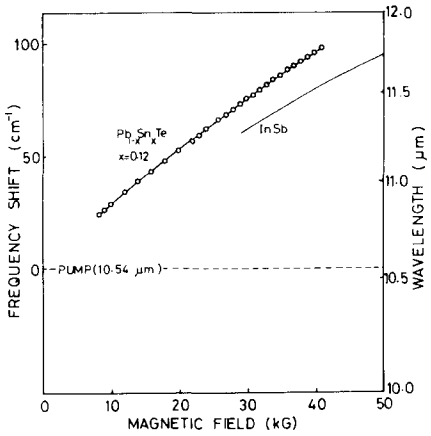

FIG. 2. Wavelength of the Stokes output and frequency shift from the pump wavelength at 10.54 μm as a function of magnetic field.

$cm^{-1}/W\ cm^{-2}$ and a threshold input power density of the stimulated emission of 0.6 MW/cm^2, the threshold Raman gain in $Pb_{0.88}Sn_{0.12}Te$ can be estimated to be about 6 cm^{-1}. However, the estimation of the absorption coefficient in the $Pb_{0.88}Sn_{0.12}Te$ cavity at 10.54 μm in the same experimental arrangement gave an approximate magnitude of 35 cm^{-1}; this fact suggests the occurrence of resonance enhancement of the Raman gain in the SFR cavity. When an absorption loss of 35 cm^{-1} and a threshold input power density of 0.6 MW/cm^2 are assumed, the Raman gain per unit input power density can be estimated to be at least $6\times10^{-5}\ cm^{-1}/W\ cm^{-2}$. The resonance enhancement factor of 6 is attained; this is quite plausible in light of the experiment on the resonance enhancement of spontaneous SFR cross section in InSb.[6]

The wavelength of the Stokes signal or the frequency shift from the 10.54-μm pumping light as a function of magnetic field is shown in Fig. 2, where our experimental curve of the InSb cavity[7,8] is also shown for comparison. The Stokes output was detectable in the magnetic field range between 8 and 41 kG, as seen in Fig. 2, because of strong dependence of the output on magnetic field (Fig. 3). The tunability of the present SFR laser is weakly dependent upon the magnetic field; a typical value is 2.3 cm^{-1}/kG. The value of effective level splitting factor (effective g factor) estimated from the slope of the curve in Fig. 2 varies from 50 to 64 depending on the magnetic field, for example, 56 at 20 kG. These values are larger than that of InSb[1,2,8] but smaller than that of $Hg_{0.77}Gd_{0.23}Te$.[4,5] The magnitude of the effective g factor is sensitive to magnetic field and electron density. Figure 2 shows clearly that the effective g factor becomes smaller with increasing magnetic field. The effective g factor tends to decrease as the electron density is increased.[9] For InSb, the effective g factor changes from 51 to 44 in the range from 10^{13} to $2\times10^{16}\ cm^{-3}$.[9] The similar dependence of the effective g factor on the electron density is likely to occur in $Pb_{1-x}Sn_xTe$. A much higher effective g factor than those observed in the present experiment can be expected in purer crystals. In fact, an effective g factor of 69 at the band edge has been experimentally observed in $Pb_{0.84}Sn_{0.16}Te$ at 47 K.[10] Moreover, Patel and Slusher[11] have found from a SFR scattering experiment that the effective g factor of a PbTe crystal with an electron density of $8\times10^{16}\ cm^{-3}$ is very dependent on the crystal orientation and is 35.5 for a magnetic field parallel to the $\langle100\rangle$ axis.

The Stokes output power varied with magnetic field as shown in Fig. 3, where three different wavelengths, 10.53, 10.49, and 10.33 μm, with a constant peak power of 100 kW, were used as the pump. Each curve shows a maximum at a slightly different magnetic field. The maximum output power decreases with increasing photon energy of the pump. The SFR laser output is strongly dependent on gain and loss mechanisms and their relative magnitude. The gain and loss factors in the $Pb_{1-x}Sn_xTe$ cavity are critically influenced by magnetic field strength and pump wavelength. Because of poor knowledge of the band parameters and magneto-optical properties of $Pb_{1-x}Sn_xTe$, it is very hard to interpret the result of Fig. 3 in a straightforward manner. We would like to attempt a qualitative argument in the following.

The energy gap of the $Pb_{1-x}Sn_xTe$ crystal is estimated to be 122 meV at 10 K at zero magnetic field.[10] The energy gap of semiconductors is generally sensitive to the application of a magnetic field. However, in the case of $Pb_{1-x}Sn_xTe$, the increase of the energy gap defined by the energy separation between the lowest conduction band level and highest valence band level is rather small because of the large effective mass and large effective g factor. For a $Pb_{0.88}Sn_{0.12}Te$ crystal the energy gap increase is to be at most only 1 meV at 20 kG.[14] The pump wavelengths, 10.53 (117.7 meV), 10.49 (118.7 meV), and 10.33 μm (120.0 meV), is much too close to the energy gap at 20 kG of 123 meV; the resonance enhancement of the Raman cross section with decreasing pump wavelength is exceeded by the increase in the loss resulting from band-edge absorption. Thus, the SFR output is decreased as the pump wavelength is decreased, as seen in Fig. 3.

The dependence of SFR output on magnetic field is mainly determined by magnetic field dependence of the scattering coefficient and absorption loss.[13,15] The scattering co-

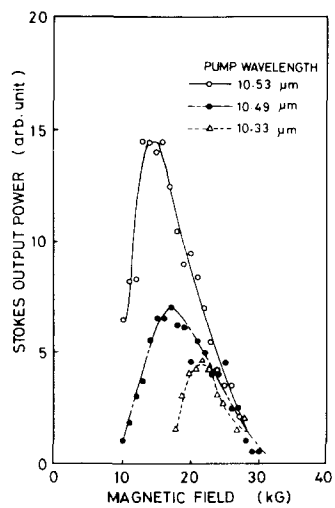

FIG. 3. Magnetic field dependence of the Stokes output power for different pump wavelengths.

efficient includes the Raman cross section and electron population in Zeeman sublevels. In a $Pb_{0.88}Sn_{0.12}Te$ crystal, the energy gap shifts only by 1 meV at 20 kG; thus, the Raman cross section shows relatively weak dependence on the magnetic field when the pump wavelength is fixed at one CO_2 laser line. The scattering coefficient is thus mostly limited by electron population in Zeeman sublevels or the position of the Fermi level.[2,12] However, due to the complexity and large nonparabolicity of the energy band in $Pb_{1-x}Sn_xTe$, the determination of the location of the Fermi level with the changing magnetic field is a hard task at present. Nevertheless, it can be said that the increase in the SFR output with increasing magnetic field from zero in Fig. 3 results from an increase in the scattering coefficient due to the change in the location of the Fermi level with magnetic field. On the other hand, in the region of the magnetic field above the peak SFR output in Fig. 3, two terms, the decrease of the scattering factor[2,13] and the increase in the absorption loss of SFR output, are operative to suppress the SFR output. Which of the two terms is essential is not clear at present. If the latter is the true process, harmonics and phonon-assisted harmonics of the cyclotron resonance[9,13] are candidates for the absorption loss. The absorption loss due to the monotonic absorption tail of magnet-plasma resonance does not seem to be dominant, because such an absorption loss increases rather gradually with increasing magnetic field and cannot interpret the steep decrease of the SFR output with magnetic field as seen in Fig. 3; further experiments on harmonic absorption of cyclotron resonance and magnet-plasma absorption at pump and SFR frequencies are necessary and are now proceeding.

The authors wish to thank Professor Y. Inuishi of Osaka University for his valuable discussion and critical reading of the manuscript.

[1]C.K.N. Patel and E.D. Shaw, Phys. Rev. Lett. **24**, 451 (1970).
[2]C.K.N. Patel and E.D. Shaw, Phys. Rev. **3**, 1279 (1971).
[3]A. Mooradian, S.R.J. Brueck, and F.A. Blum, Appl. Phys. Lett. **17**, 481 1970).
[4]B.A. Weber, J.P. Sattler, and J. Nemarich, Appl. Phys. Lett. **27**, 93 (1975).
[5]P.W. Kruse, Appl. Phys. Lett. **28**, 90 (1976).
[6]S.R.J. Brueck, A. Mooradian, and F.A. Blum, Phys. Rev. **137**, 5253 (1973).
[7]K. Yasuda, J. Shirafuji, and Y. Inuishi, Oyo-Butsuri **46**, 943 (1977) (in Japanese).
[8]H. Takamatu, K. Yasuda, J. Shirafuji, and Y. Inuishi, Tech. Rep. Osaka Univer. **26**, 437 (1976).
[9]E.J. Johnson and D.H. Dickey, Phys. Rev. B **1**, 2676 (1970).
[10]C.R. Hewes, M.S. Adler, and S.D. Senturia, Phys. Rev. B **7**, 5195 (1973).
[11]C.K.N. Patel and R.E. Slusher, Phys. Rev. **177**, 1200 (1969).
[12]B.S. Wherrett, S. Wolland, C.R. Pidgeon, R.B.Dennis, and S.D. Smith, *Proc. 12th Intern. Conf. Phys. Semicond., Stuttgalt*, 1974 (Teubner, Stuttgalt, 1974), p. 793.
[13]R.B. Dennis, W.J. Firth, A. McNeith, C.R. Pidgeon, S.D. Smith, J.W. Smith, B.S. Wherrett, and R.A. Wood, *Proc. 11th Intern. Conf. Phys. Semicond., Warsaw*, 1972 (Scientific Publishers, Warsaw, 1972), p. 364.
[14]J.F. Butler, Solid State Commun. **7**, 909 (1969).
[15]R.B. Dennis, C.R. Pidgeon, S.D. Smith, B.S. Wherrett, and R.A. Wood, Proc. R. Soc. London A **331**, 203 (1972).

The CdTe/HgTe superlattice: Proposal for a new infrared material

J. N. Schulman and T. C. McGill

California Institute of Technology, Pasadena, California 91125
(Received 12 January 1979; accepted for publication 7 March 1979)

We propose a new material which could be useful in a number of infrared optoelectronic devices. The material consists of alternating (100) layers of CdTe and HgTe. The band gap of this superlattice is adjustable from 0 to 1.6 eV depending on the thicknesses of the CdTe and HgTe layers. Details of the band-gap variation and the character of the band-edge states are presented.

PACS numbers: 85.60.Gz, 73.40. – c, 73.60.Fw

Mercury telluride and cadmium telluride are the constituents of an important group of alloys used for infrared applications.[1] The $Hg_{1-x}Cd_xTe$ alloy has band gaps which range from 0 to 1.6 eV as x is varied from zero to unity. In this letter we propose that alternating layers of CdTe and HgTe, the CdTe/HgTe superlattices, could also be an interesting material for application in infrared optoelectronic devices.

The CdTe/HgTe superlattice could be fabricated by molecular beam epitaxy (MBE). Both HgTe and CdTe crystallize in the zinc–blende structure. They are nearly lattice matched with bulk lattice constants differing by about 0.3% ($a_{HgTe} = 6.46$ Å and $a_{CdTe} = 6.48$ Å).[1] The MBE process is simplified by the fact that the anion, tellurium, is common to both. Arrangement in a superlattice allows additional flexibility over the $Hg_{1-x}Cd_xTe$ random alloy in adjusting the band gap for a given Cd-to-Hg ratio. This structure may be more stable than the random alloy, with the structural defects reduced due to the spatial separation of the HgTe and CdTe in distinct bulklike layers.

In this letter we report the results of a theoretical study of this superlattice formed by alternating layers parallel to

 0003-6951/79/100663-03$00.50